A Permeant Ion Binding Site Located between Two Gates of the *Shaker* K^+ Channel

R. E. Harris, H. P. Larsson, and E. Y. Isacoff
Department of Molecular and Cell Biology, University of California, Berkeley, Berkeley, California 94720-3200 USA

ABSTRACT K^+ channels can be occupied by multiple permeant ions that appear to bind at discrete locations in the conduction pathway. Neither the molecular nature of the binding sites nor their relation to the activation or inactivation gates that control ion flow are well understood. We used the permeant ion Ba^{2+} as a K^+ analog to probe for K^+ ion binding sites and their relationship to the activation and inactivation gates. Our data are consistent with the existence of three single-file permeant-ion binding sites: one deep site, which binds Ba^{2+} with high affinity, and two more external sites whose occupancy influences Ba^{2+} movement to and from the deep site. All three sites are accessible to the external solution in channels with a closed activation gate, and the deep site lies between the activation gate and the C-type inactivation gate. We identify mutations in the P-region that disrupt two of the binding sites, as well as an energy barrier between the sites that may be part of the selectivity filter.

INTRODUCTION

In 1955 Hodgkin and Keynes proposed that K^+ channels have long pores that can simultaneously hold multiple permeant ions as they flux in single file. This model has been expanded to the point where it is now believed that before entering the pore, each K^+ ion in solution must first shed its waters of hydration to pass through the narrowest region. As waters of hydration are shed, K^+ ions make intimate interactions with pore-lining residues at what are thought to be discrete ion binding sites (Hille, 1992). Attempts to locate the structural determinants of the K^+ channel pore have provided evidence that the P-region (original mutagenesis: MacKinnon and Yellen, 1990; Hartmann et al., 1991; Yellen et al., 1991; Yool and Schwarz, 1991; Heginbotham et al., 1992; Kirsch et al., 1992; toxin binding: MacKinnon and Miller, 1989; MacKinnon et al., 1990; Goldstein et al., 1994; Aiyar et al., 1995; Hidalgo and MacKinnon, 1995; Naranjo and Miller, 1996; Ranganathan et al., 1996), the internal S4-S5 loop (Isacoff, 1991; Slesinger, 1993), and S6 (Choi et al., 1993; Isacoff et al., 1993; Aiyar et al., 1994; Lopez et al., 1994; Taglialatela et al., 1994) form the pore. A flux ratio experiment indicates that at least four K^+ ion binding sites are located within these regions of the *Shaker* potassium channel (Stampe and Begenisich, 1996). The narrowest region, which determines ion selectivity, is localized to the highly conserved "signature sequence" within the P-region (Heginbotham et al., 1992, 1994; cysteine probing: Kurz et al., 1995; Lu and Miller, 1995; Pascual et al., 1995). Residues in and near this "signature sequence" have been identified that may form ion binding sites (Yellen et al., 1991; Heginbotham and MacKinnon, 1992; Kirsch et al., 1992; Choi et al., 1993; Ranganathan et al., 1996) or act as barriers to ion movement (Harris and Isacoff, 1996; Hurst et al., 1996).

The extremely fast (10^7–10^8/s) flux rate of K^+ through the pore has made it difficult to study K^+ ion binding at these sites. This problem was mainly overcome in a study of the large-conductance calcium-activated (BK) K^+ channel by Neyton and Miller (1988a, b) through the use of Ba^{2+}. Ba^{2+}, a permeant ion with the same crystal diameter as K^+, binds in the channel with a dwell time 10^6 longer than that of K^+, which is long enough for its occupancy to be measured as a block of K^+ flux. By examining the influence of K^+ ions on Ba^{2+} dissociation, Neyton and Miller defined both the electrical location and affinity of three K^+ ion binding sites in the BK pore.

In this study, we have applied the method developed by Neyton and Miller to characterize three permeant ion binding sites in the pore of the voltage-gated *Shaker* K^+ channel, which we find to closely resemble those of the BK channel. We identified pore-lining residues that appear to contribute to the formation of the two deeper sites, and ask where the sites are located with respect to the channel gates. Interestingly, we found that the deepest of the three sites binds ions most tightly, is located between the activation gate and the C-type inactivation gate, and can be occupied when either of these gates is closed. In this respect, the C-type inactivation gate is similar to the activation gate studied by Armstrong (Armstrong and Hille, 1972), in that it can close on a pore blocker that is bound in the pore. These results are consistent with a mechanism of gating that operates by pinching off access of the deep pore to the internal or external solution.

Received for publication 28 August 1997 and in final form 19 December 1997.

Address reprint requests to Dr. Ehud Y. Isacoff, Department of Molecular and Cell Biology, Division of Neurobiology, University of California, 271 Life Science Addition, Berkeley, CA 94720. Tel.: 510-642-9853; Fax: 510-643-6791; E-mail: ehud@uclink.berkeley.edu.

Dr. Larsson's present address is The Nobel Institute for Neurophysiology, Department of Neuroscience, Karolinska Institutet, S-171 77 Stockholm, Sweden.

0006-3495/98/04/1808/13 $2.00

MATERIALS AND METHODS

Molecular biology

All experiments were performed on the N-terminal deleted (6-46) ShBΔ (Hoshi et al., 1990) channel and mutants that were made in this background. The gene had been cloned into pBluescript (Stratagene) + vector. Mutant plasmids were generated by the *dut-ung*-procedure as described by Sambrook et al. (1989). Plasmids were transformed into DH5α cells, and dsDNA was isolated by an alkaline lysis procedure. Mutant plasmids were sequenced by the Sanger dideoxy method. Dimethyl capped cRNA was prepared from mutant and wild-type plasmids by *in vitro* runoff transcription reactions, using either Ambion (Megascript) or Stratagene transcription kits with T7 RNA polymerase after linearization with *Hin*dIII. RNA pellets were resuspended in ultrapure water (Specialty Media, Laballette, NJ), and yields were determined by formaldehyde-agarose gel electrophoresis. Aliquots were stored at −80°C until needed for oocyte injection.

Electrophysiology

Stage V and VI *Xenopus laevis* oocytes were isolated, collagenased (Worthington Biochemical Corp.), and stored at 18°C in MBSH solution. MBSH contained (in mM) 88 NaCl, 1.0 KCl, 2.4 $NaHCO_3$, 10 HEPES (pH 7.5 with NaOH), 0.82 $MgSO_4$ (7 H_2O), 0.33 Ca $(NO_3)_2$ (4 H_2O), 0.41 $CaCl_2$ (2 H_2O). Pyruvate (2.5 mM final concentration), penicillin-streptomycin, gentamicin, 0.5 g bovine serum albumin (per liter), and 0.5 g Ficoll (per liter) were also added. After isolation, 50–100 nl of cRNA was injected into each oocyte, and recordings were made 2–6 days after injection.

Electrodes (0.2–1 mΩ) were pulled on a model P-87 Flaming/Brown micropipette puller (Sutter Instrument Company) and filled with 3 M KCl. After recording, any drift of the electrode voltage offset relative to the bath solution was noted upon removal of the voltage electrode from the oocyte. Recordings with over 5-mV drift were excluded. All external solutions contained 10 mM HEPES (pH to 7.0 with either KOH or NaOH, depending on which was the major cation in solution) and 0.41 mM $CaCl_2$. The 2 mM KCl solution contained (in mM) 112 NaCl and 2 KCl. The 112 mM KCl solution contained 112 mM KCl. The 10 mM Ba^{2+} "low K^+" solution contained (in mM) 10 $BaCl_2$, 2 KCl, and 92 NaCl. The 10 mM Ba^{2+} "high K^+" solution contained 10 mM $BaCl_2$ and 92 mM KCl. The 0 mM K^+ solution contained 112 mM NaCl. All recordings were made at room temperature (21–23°C).

Oocytes were typically held at −80 mV, except where stated otherwise in the text, and stepped to test potentials. The duration of test voltages was 800 ms for the experiments measuring open channel Ba^{2+} dissociation and 30 ms for experiments containing both closed and open channels (closed/open). Leak currents were subtracted on line with a P/4 subtraction protocol for the closed/open channel experiments. No leak subtraction was done for the open channel Ba^{2+} dissociation experiments. Data were acquired with an Axoclamp-2A amplifier (Axon Instruments, Foster City, CA), a TL-1 AD/DA computer interface (Axon Instruments, Foster City, CA), and an IBM 486 AST PC. Data were sampled at 1 or 5 kHz and filtered first through a 1-pole low-pass filter (Axoclamp-2A) at 30 kHz, and then filtered again at 200 Hz or 1 kHz through an 8-pole Bessel filter (Frequency Devices). Data were analyzed with pClamp software (Axon Instruments). To determine the time course of Ba^{2+} wash-out from open channels in the presence of significant C-type inactivation (such as with 0 K^+_{out}), a control trace acquired in the absence of Ba^{2+} was subtracted from the experimental trace exhibiting Ba^{2+} unbinding.

Model of Ba^{2+} open channel dissociation

The voltage dependence of open-channel Ba^{2+} dissociation was modeled with a single-file three permeant ion binding site model (Fig. 3 *C*). Site 1 is the "lock-in" site and the shallow fast equilibrating Ba^{2+} block site. Site 2 is the low-affinity "enhancement" site. Site 3 is the deep Ba^{2+} binding site. The total off rate for Ba^{2+} from site 3 of open channels is equal to the off rate in the outward direction plus the off rate in the inward direction:

$$K_{\text{off total}} = \alpha_{v,c} + \beta_{v,c} \tag{1}$$

where $\alpha_{v,c}$ is the off rate for Ba^{2+} in the outward direction, and $\beta_{v,c}$ is the off rate for Ba^{2+} in the inward direction. Both of these rate constants are dependent on membrane voltage (v) and external K^+ concentration (c).

The Ba^{2+} off rate in the outward direction can be expressed as

$$\alpha_{v,c} = [1 - (f_1(v, c) + f_2(v, c) + f_{1+2}(v, c))] \times \alpha_0 \times \exp(\delta_{\alpha\text{off}} 2FV/RT) \tag{2}$$

where $f_1(v, c)$ is the fraction of channels with site 1 occupied by an external K^+ ion, $f_2(v, c)$ is the fraction of channels with only site 2 occupied by a K^+ ion, and $f_{1+2}(v, c)$ is the fraction of channels with both sites 1 and 2 occupied by K^+ ions. α_0 is the outward off rate at 0 mV, and $\delta_{\alpha\text{off}}$ is the electrical distance from the Ba^{2+} binding site to the rate-limiting barrier to Ba^{2+} exit in the outward direction. *F, V, R,* and *T* have their usual meanings. The same equation written with the fractional states occupancies, f_x, expressed explicitly in terms of binding constants, becomes

$$\alpha_{v,c} = (1 + c/k_1 + c/k_1 \times k_2 + c^2/k_1 \times k_2 \times k_3)^{-1} \times \alpha_0 \times \exp(\delta_{\alpha\text{off}} 2FV/RT) \tag{3}$$

where

$$k_1 = k_{1(0\text{ mV})} * \exp(\delta_1 FV/RT)$$

$$k_2 = k_{2(0\text{ mV})} * \exp(\delta_2 FV/RT)$$

$$k_3 = k_{3(0\text{ mV})} * \exp(\delta_3 FV/RT)$$

and where $k_{1(0\text{ mV})}$ is the dissociation constant at 0 mV membrane potential for K^+ binding to site 1 (when Ba^{2+} occupies site 3), δ_1 is the electrical distance for K^+ to bind to site 1 from the external solution (fixed at 0.18 based upon the δ of fast Ba^{2+} block; see below), $k_{2(0\text{ mV})}$ is ratio of the number of channels with site 1 occupied by K^+ to the number of channels with K^+ occupying site 2 at 0 mV, δ_2 is the electrical distance from site 1 to site 2, $k_{3(0\text{ mV})}$ is the dissociation constant at 0 mV membrane potential for K^+ to bind at site 1 when there is a K^+ ion at site 2, and δ_3 is the electrical distance for K^+ to bind at site 1 when site 2 is occupied by a K^+ ion. For simplicity, $\delta_1 = \delta_3$.

The rate of Ba^{2+} dissociation in the inward direction can be expressed as

$$\beta_{v,c} = (1 - f_{1+2}(v, c)) \times \beta_0 \times \exp(-\delta_{\beta\text{off}} 2FV/RT) + f_{1+2}(v, c) \times \beta_0' \times \exp(-\delta_{\beta'\text{off}} 2FV/RT) \tag{4}$$

where β_0 is the dissociation rate at 0 mV in the inward direction for Ba^{2+} when site 1 or site 2 is occupied by K^+ or when both sites are unoccupied by K^+. We set this value to zero because there is little inward dissociation with 0 mM K^+_{out} and 2 mM K^+_{out} (Fig. 2 *C*). β_0' is the Ba^{2+} off rate in the inward direction at 0 mV when sites 1 and 2 are occupied by K^+. $\delta_{\beta'\text{off}}$ is the electrical distance from the Ba^{2+} ion binding site to the rate-limiting barrier to its exit in the inward direction. The same equation written with the fractional states occupancies, f_x, expressed explicitly in terms of binding constants, becomes

$$\beta_{v,c} = (c^2/k_1 \times k_2 \times k_3) \times (1 + c/k_1 + c/k_1 \times k_2 + c^2/k_1 \times k_2 \times k_3)^{-1} \times \beta_0' * \exp - (\delta_{\beta'\text{off}} 2FV/RT) \tag{5}$$

Therefore the total Ba^{2+} off rate (Eq. 1) expressed in terms of external K^+ concentration and voltage is simply the sum of Eqs. 3 and 5. The Ba^{2+} ion dissociation rates for 0 mM K^+, 2 mM K^+, and 112 mM K^+ were fit simultaneously (Madonna 5.1.2) with the sum of Eqs. 3 and 5, yielding the

solid line fits in Fig. 3 *B*. The four fixed parameters were α_0 (6.77 s^{-1}), $\delta_{\alpha off}$ (0.355), δ_1 (0.18), and δ_3 (0.18). α_0 and $\delta_{\alpha off}$ were determined from experiments, respectively, as the 0 mV off rate and $\delta_{\alpha off}$ for Ba^{2+} with 0 mM K^+_{out}. δ_1 was assumed to be 0.18, the voltage dependence of external Ba^{2+} binding to its fast site (see below), which is site 1 in the model. For simplicity, $\delta_1 = \delta_3$. The values for the free parameters derived from a fit of the model to the data (Fig. 3 *B*) were

$$\beta_0' = 3.74 \times 10^3\ s^{-1}$$

$$\delta_{\beta' off} = 0.337$$

$$k_1 = 7.49 \times 10^{-4}\ M$$

$$k_2 = 5.47 \times 10^3$$

$$k_3 = 6.40 \times 10^{-4}\ M$$

$$\delta_2 = 0.130$$

Model for Ba^{2+} block

The calculation of the voltage dependence of Ba^{2+} unblock in Fig. 5 *C* required a model for Ba^{2+} blockade. In our model channels are in one of three possible states:

$$O \underset{\beta}{\overset{[Ba^{2+}]_\alpha}{\rightleftharpoons}} B_1 \underset{\gamma}{\overset{\epsilon}{\rightleftharpoons}} B_3$$

where O is the unblocked conducting state of the channel, B_1 is Ba^{2+} bound to the fast site (site 1), and B_3 is Ba^{2+} bound to the slow site (site 3). (Site 2 is the low-affinity site, which we assume is occupied minimally under 10 mM Ba^{2+}.) α, β, γ, and ϵ are rate constants. Differential equations for the disappearance of these states can be written and solved for at equilibrium. This yields the following equations:

$$O/B_1 = \beta/\alpha[Ba^{2+}] = K_{d_{fast}} \times e^{(\delta_{fast} FV2/RT)}/[Ba^{2+}] \quad (6)$$

$$B_1/B_3 = \gamma/\epsilon = K \times e^{(\delta_{13} FV2/RT)} \quad (7)$$

where δ_{fast} is the electrical distance to site 1 from the external solution, δ_{13} is the electrical distance between site 1 and site 3, $K_{d_{fast}}$ is the $K_{d(0\ mV)}$ for Ba^{2+} at site 1, and K is the 0 mV equilibrium constant for Ba^{2+} movement between sites 1 and 3. Using Eq. 6, one can calculate the fraction unblocked for site 1:

$$O/(O+B_1) = (1 + [Ba^{2+}]e^{-\delta_{fast} FV2/RT}/K_{d_{fast}}) - 1$$

A fit of the voltage dependence of the fraction unblocked for site 1 to the observed fraction unblocked of the fast component (Fig. 5, *A* and *C*) gives the values of $K_{d_{fast}}$ (10.0 mM) and δ_{fast} (0.18). The fast component of block was measured as in Fig. 5 *A* (fraction unbound of the fast component = 1 − fast). Obtaining δ_{13} and the $K_{d_{(0\ mV)}}$ for site 3 is more complex and requires calculation of the total fraction of unblocked channels. Using Eqs. 6 and 7, the total fraction of unblocked channels is

$$O/(O + B_1 + B_3) = (1 + [Ba^{2+}]e^{-\delta_{fast} FV2/RT}/K_{d_{fast}} + [Ba^{2+}]e^{-\delta_{slow} FV2/RT}/K_{d_{slow}})^{-1} \quad (8)$$

where $K_{d_{slow}}$ is $KK_{d_{fast}}$, which is the $K_{d(0\ mV)}$ for the slow site (site 3), and δ_{slow} is $\delta_{fast} + \delta_{13}$, which is the electrical distance between the external solution and site 3. The total fraction of unblocked channels was measured as in Fig. 5 *A* (total unblocked = 1 − fast − slow). This data were plotted against step potential and fit with Eq. 9 (Fig. 5 *C;* total unblocked). The fit gives the values for $K_{d_{slow}}$ (1.11 mM) and δ_{slow} (0.38), using the values of $K_{d_{fast}}$ and δ_{fast} obtained above from the fit of Eq. 8 to the observed fraction unblocked of the fast component. For simplicity, we have ignored K^+ binding to sites 1 and 3. This experiment could not be carried out in K^+-free solutions because we find that Ba^{2+} increases current in K^+-free solutions before blocking conductance (data not shown).

To compare the effect of the mutations on the fast and slow components of Ba^{2+} block (Fig. 7), the fractions unblocked for the fast and slow components were calculated for both wild-type and mutant channels as follows. The fraction unblocked for the fast component was calculated as above (fraction unblocked fast = 1 − fast; Fig. 5 *A*). The fraction unblocked of the slow component was taken as the fractional amount of current at steady state of the slow component divided by the amount of current after fast block (fraction unblocked slow = unblocked/slow + unblocked; Fig. 5 *A*).

RESULTS

Open-channel Ba^{2+} dissociation

At negative voltages, external Ba^{2+} entered the pore of N-terminal deleted *Shaker* channels (ShBΔ; Hoshi et al., 1990) and remained bound after wash-out of Ba^{2+} from the external solution, as measured by a depolarizing step after the wash-out (Fig. 1 *A*). This depolarization evoked current from a fraction of the channels at the normal opening rate, whereas the bulk of the current rose much more slowly, consistent with the idea that the majority of channels were open, but blocked by Ba^{2+}, and that they then slowly became unblocked (Fig. 1 *B*). The open channel Ba^{2+} off rate was taken as the reciprocal of the time constant for the slow rising phase, which was fit well by a single exponential. In all of our analysis, we assume that the channel gates

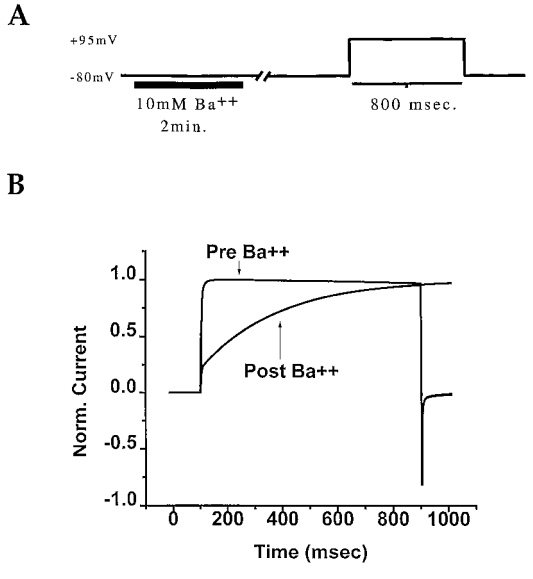

FIGURE 1 Open channel Ba^{2+} dissociation from wild-type ShBΔ channels. (*A*) The Oocyte was held at −80 mV as the perfusing bath solution was switched from 0 mM Ba^{2+}/112 mM K^+ to 10 mM Ba^{2+}/2 mM K^+/92 mM Na^+ and back to 0 mM Ba^{2+}/112 mM K^+ while holding at −80 mV. Two minutes after Ba^{2+} wash-out, a 800-ms depolarizing step opened the channels. (*B*) Current traces are in response to a 800-ms step to +95 mV before and after perfusion of 10 mM Ba^{2+}. The post-Ba^{2+} trace contains a fast component reflecting opening of channels that were unbound to Ba^{2+}, and a slow component reflecting Ba^{2+} unbinding from open channels. The slow component was fit with a single exponential, τ_{off} = 280 ms.

normally with a Ba^{2+} bound in the pore (but see Miller et al., 1987; Neyton and Pelleschi, 1991).

These observations in the ShBΔ channel are consistent with those found in the delayed rectifier K^+ channel of squid giant axon (Armstrong et al., 1982), in which external Ba^{2+} enters the closed channel at negative voltages, binds at a deep high-affinity site, and is prevented from dissociating inwardly by the closed activation gate and outwardly by the electric field. These results are also similar to observations in the BK channel, where Ba^{2+} can be trapped in the channel when closure of the activation gate prevents its inward dissociation (Miller, 1987).

Dependence of open-channel Ba^{2+} dissociation on voltage and external K^+

In 0 mM [K^+_{out}], the rate of open channel Ba^{2+} dissociation increased with increasingly depolarized step potentials (Fig. 2, *A* and *C*), suggesting that at positive potentials Ba^{2+} dissociated primarily in the outward direction. The electrical distance from the Ba^{2+} ion binding site to its rate-limiting barrier for exit, δ_{off} (Woodhull, 1973), was 0.35, indicating that the binding site lies deep in the membrane electric field. Increasing [K^+_{out}] from 0 mM to 2 mM slowed Ba^{2+} dissociation at all voltages studied, with little effect on δ_{off} (δ_{off} = 0.373; Fig. 2, *B* and *C*). The slowing of Ba^{2+} dissociation by external K^+ (by threefold at 0 mV) suggests that a more external K^+ ion binding site must be empty for outward Ba^{2+} dissociation. This behavior is very similar to that described for K^+ occupancy of the high-affinity "lock-in" site seen in BK channels (Neyton and Miller, 1988a).

Ba^{2+} dissociation was very different when the external concentration of [K^+] was raised to 112 mM. At this high external K^+ concentration, the rate of Ba^{2+} dissociation slowed with increased depolarization between +20 mV and +100 mV, and then increased at more positive potentials (Fig. 3, *A* and *B*). This suggests that in 112 mM [K^+_{out}], Ba^{2+} has a propensity to dissociate in the inward direction, but at extreme depolarizations the electric field becomes strong enough to reverse this trend and drive Ba^{2+} outward. This behavior is very similar to that described for the "enhancement" site in BK channels that binds K^+ with low affinity (Neyton and Miller, 1988b).

These observations indicated that, like BK, the deep pore of *Shaker* has three binding sites that are in ready exchange with the external solution: a deep Ba^{2+} binding site and two shallower sites, one with low affinity ("enhancement" site) and the other with higher affinity ("lock-in" site) for K^+ in the Ba^{2+} bound channel.

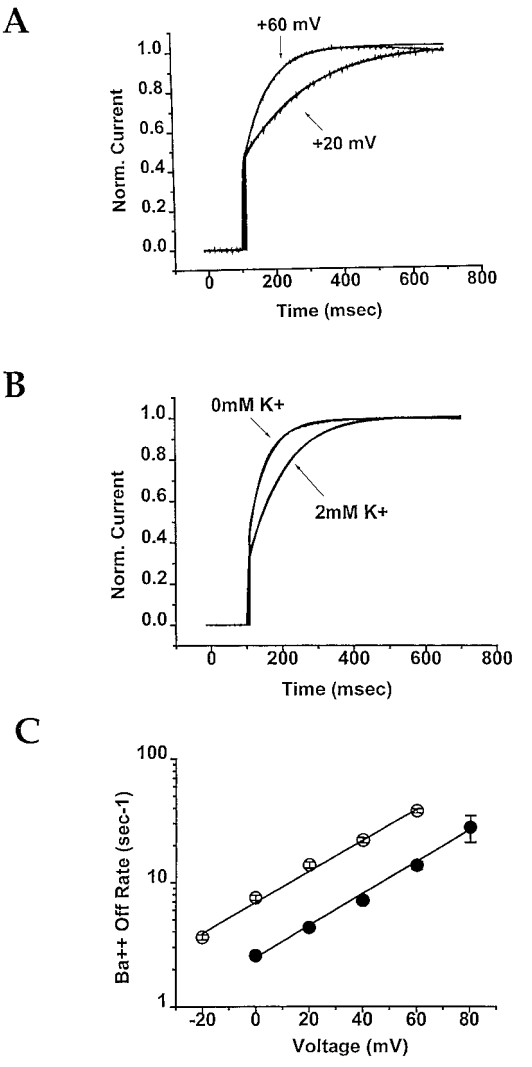

FIGURE 2 Ba^{2+} dissociation from wild-type ShBΔ open channels is dependent on voltage and external K^+ concentration. (*A*) Post-Ba^{2+} currents at two step potentials in 2 mM K^+_{out}. The slow components of the traces were fit with single exponentials. The +60-mV trace (τ_{off} = 72.0 ± 4.43 ms, n = 12) was significantly faster ($p = 3.01 \times 10^{-10}$) than the +20-mV trace (τ_{off} = 210 ± 11.6 ms, n = 16), suggesting outward Ba^{2+} dissociation in 2 mM K^+_{out}. (*B*) Post-Ba^{2+} current in 0 mM K^+_{out} (τ_{off} = 44.4 ± 8.83 ms, n = 4) was significantly faster ($p < 1 \times 10^{-4}$) than 2 mM K^+_{out} (τ_{off} = 130 ± 8.83 ms, n = 12), V_{step} = +40 mV. (*C*) Voltage dependence of open channel Ba^{2+} off rates for 0 mM K^+_{out} (○) and 2 mM K^+_{out} (●). Lines are fits to the equation $K_{off} = K_{off(0\ mV)}$*exp($z\delta_{off}FV/RT$), where $K_{off(0\ mV)}$ is the off rate with no applied voltage, δ_{off} is the electrical distance from the Ba^{2+} binding site to the rate-limiting barrier to Ba^{2+} exit, z is the valence of Ba^{2+}, and *F, R,* and *T* have their usual meanings. The 0 mV Ba^{2+} off rates are 6.65 s^{-1} for 0 mM K^+_{out} and 2.40 s^{-1} for 2 mM K^+_{out}. δ_{off} is 0.348 for 0 mM K^+_{out} and 0.373 for 2 mM K^+_{out}.

Ion selectivity of the "lock-in" site

To examine the selectivity of the "lock-in" site, the 0 mV Ba^{2+} off rate was determined with different external ions at the low (2 mM) concentration (Fig. 4 *A*). Compared to 112 mM Na^+_{out}, the 0 mV Ba^{2+} off rate was not slowed by 2 mM NH_4^+, but was slowed threefold by 2 mM K^+, and sevenfold by 2 mM Rb^+. Replacement of 112 mM Na^+ with 112 mM $NMDG^+$, a large cation that presumably does not bind to the pore, increased the Ba^{2+} off rate by 1.5-fold. This indicates that Na^+ itself bound to the "lock-in" site, but so weakly that it had an effect smaller than that of K^+ at 56 times the concentration. The affinity series for the "lock-in"

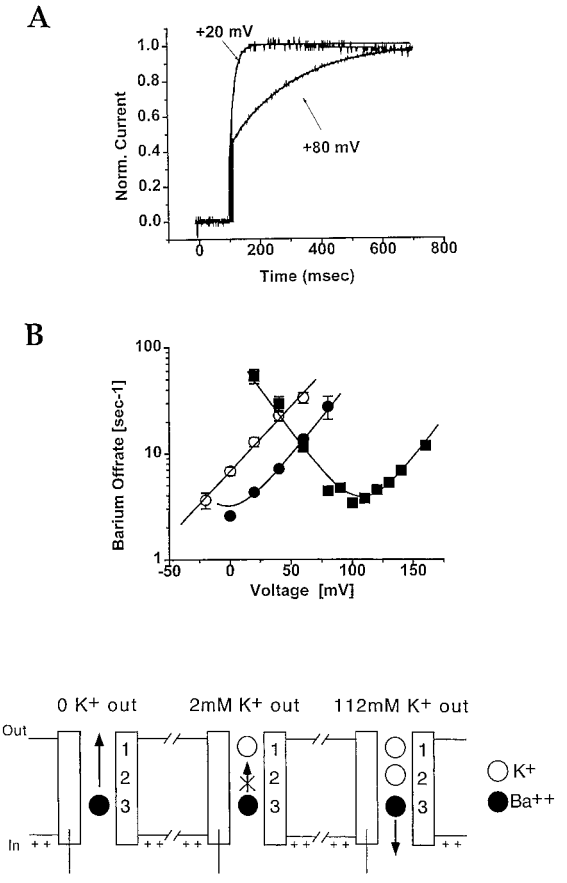

FIGURE 3 Ba^{2+} dissociates in the inward direction in 112 mM K^+_{out}. (*A*) Post-Ba^{2+} traces are shown for steps to +20 mV and +80 mV step potentials in 112 mM K^+_{out}. The time constants for Ba^{2+} dissociation were 20.3 ± 2.87 ms (n = 5) at +20 mV and 228 ± 5.49 ms (n = 4) at +80 mV ($p = 3.52 \times 10^{-9}$). (*B*) Voltage dependence of Ba^{2+} off rates are plotted against the step potential for 0 mM K^+_{out} (○), 2 mM K^+_{out} (●), and 112 mM K^+_{out} (■). The lines are simultaneous fits to a model with three permeant ion binding sites (see Materials and Methods and panel), where Ba^{2+} outward dissociation from the deep site, site 3, is prevented when a K^+ ion is located at the external "lock-in" site, site 1, and Ba^{2+} dissociation is speeded up in the internal direction when K^+ ions occupy the "lock-in" site and the "enhancement" site, site 2, simultaneously. (*C*) A diagrammatic model of Ba^{2+} dissociation from its deep site is shown. In 0 mM K^+_{out}, Ba^{2+} dissociates more easily in the outward than in the inward direction. In 2 mM K^+_{out}, K^+ sometimes is bound to the "lock-in" site, preventing outward Ba^{2+} dissociation. In 112 mM K^+_{out}, K^+ ions occupy the "lock-in" site and the "enhancement" site (which has lower affinity for K^+ because of repulsion by Ba^{2+} at the deep site 3), and Ba^{2+} is repelled in the inward direction.

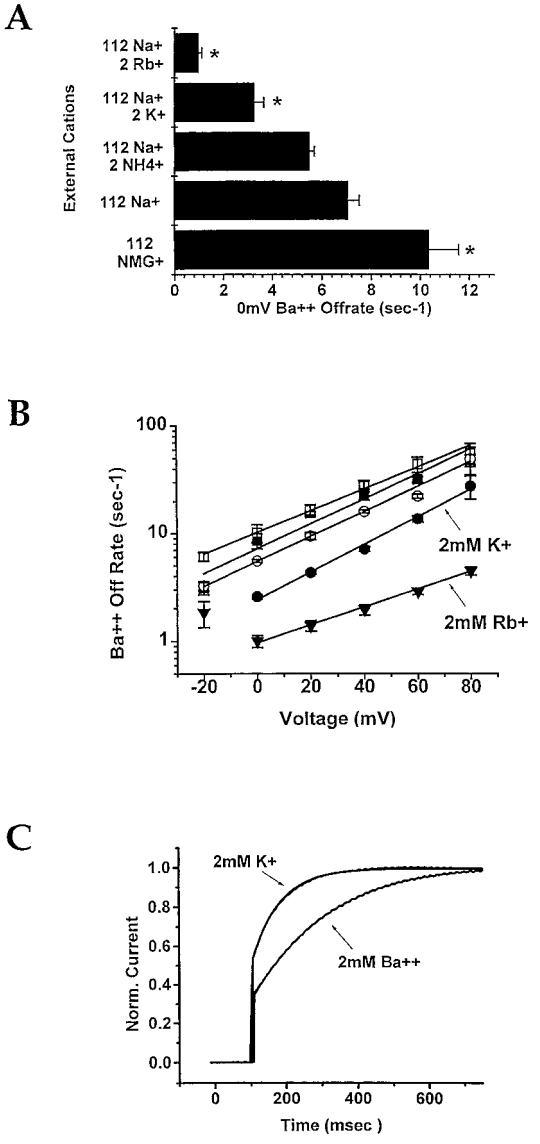

FIGURE 4 Ion selectivity of the "lock-in" site. (*A*) Ba^{2+} off rates at 0 mV with different external ions. Values of the mean off rates are for 112 mM $NMDG^+$: 10.4 ± 1.20 s^{-1} (n = 6); 112 mM Na^+: 7.06 ± 0.450 s^{-1} (n = 23); 2 mM NH_4^+/112 mM Na^+: 5.51 ± 0.182 s^{-1} (n = 3); 2 mM K^+/112 mM Na^+: 3.27 ± 0.383 s^{-1} (n = 12); and 2 mM Rb^+/112 mM Na^+: 1.00 ± 0.125 s^{-1} (n = 3). Stars represent values that are significantly different ($p < 0.05$) from 112 mM Na^+ by t-test. (*B*) Ba^{2+} off rates are plotted against step potential for different external ion concentrations. δ_{off} values are 0.293 for 112 mM $NMDG^+$ (□), 0.335 for 112 mM Na^+ (■), 0.337 for 2 mM NH_4^+/112 mM Na^+ (○), 0.373 for 2 mM K^+/112 mM Na^+ (●), and 0.239 for 2 mM Rb^+/112 mM Na^+ (▲). (*C*) Post 10 mM Ba^{2+} traces are shown for 2 mM K^+_{out} and 2 mM Ba^{2+}_{out}. Values of τ for 2 mM K^+ and 2 mM Ba^{2+} are 59.3 ± 6.01 ms (n = 9) and 145 ± 11.1 ms (n = 7), respectively ($p < 1 \times 10^{-5}$). V_{step} = +80 mV.

site was, therefore, $Rb^+ > K^+ \gg Na^+ > NMDG^+$. This series is identical to the BK channel studied by Neyton and Miller (1988a). The high selectivity of the "lock-in" site for permeant ions suggests that this site lies in the pore. Changing the external ion concentration had little effect on δ_{off}, except in the case of Rb^+ (Fig. 4 *B*).

Ba^{2+}_{out} (2 mM) was also found to bind to the "lock-in" site and slow the outward dissociation of a second Ba^{2+} bound at the deep binding site (Fig. 4 *C*). In 2 mM external Ba^{2+}, Ba^{2+} can associate with its deep site in channels that are not blocked, which should accelerate the slow rise phase of current, because $\tau = 1/[Ba^{2+}]\alpha + \beta$ (where α = on rate and β = off rate) compared to 0 Ba^{2+} during the washout, where $\tau_{off} = 1/\beta$. However, because the rise of current was slower in 2 mM Ba^{2+}_{out} than that in 2 mM K^+_{out}, it seems instead that a Ba^{2+} ion located at the "lock-in" site was able to slow the dissociation of a second Ba^{2+} at the deep site.

This effect was similar to the effect of monovalent ions at low concentration, in that greater depolarization accelerated Ba^{2+} dissociation ($\tau = 406 \pm 28.0$ ms $V_{step} = +20$ mV $n = 8$; $\tau = 145 \pm 11.1$ s $V_{step} = +80$ mV $n = 7$). This suggests that external Ba^{2+}, like external K^+, can bind at the "lock-in" site and block outward dissociation of a second Ba^{2+} bound at the deep high-affinity blocking site.

Electrical location of Ba^{2+} binding sites

To determine the relative locations within the electric field of the two Ba^{2+} binding sites, we examined the rates with which external Ba^{2+} reached and dissociated from them. Short repeated depolarizations applied during the wash-in of 10 mM external Ba^{2+} revealed two kinetic components of block onset, each representing about half of a total of 80% block (Fig. 5 *A*). The fast component was faster than the rate of exchange of Ba^{2+} in the bath, and was rapidly reversed after short exposures to Ba^{2+} (Fig. 5 *B*), whereas longer exposures that brought the slow component to steady-state reversed more slowly. Wash-out after a long exposure contained one component. These observations are consistent with those of Hurst et al. (1995), who suggested that Ba^{2+} binds to two sites, a shallow, rapidly equilibrating site and

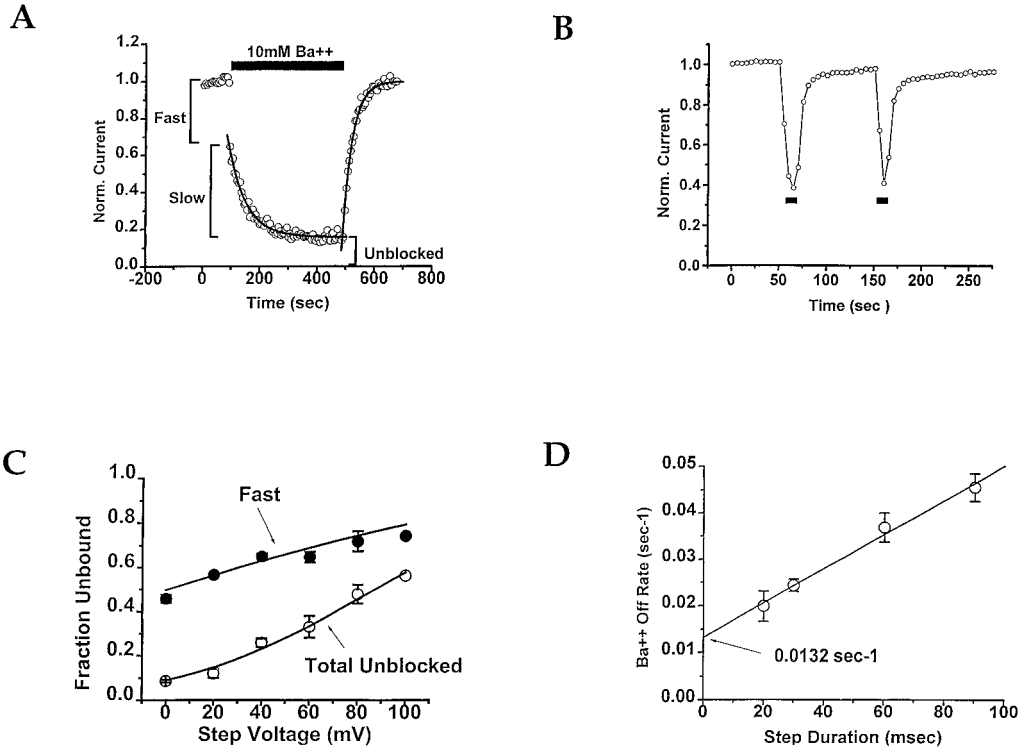

FIGURE 5 Open and closed channel Ba^{2+} block of ShBΔ. (*A*) Membrane voltage was held at −80 mV and a 30-ms step to +40 mV was made at 0.2 Hz. Steady-state current at the end of the step was normalized and plotted against time. Switching the external solution from 2 mM K^+/112 mM Na^+ to 10 mM Ba^{2+}/2 mM K^+/92 mM Na^+ led to a biphasic decay. The fast component of decay was too fast to determine its time course. The slow component of decay was well fit with a single exponential ($\tau = 90.1$ s; amp. = 0.352). Washout of Ba^{2+} was also fit well with a single exponential ($\tau = 30.8$ s; amp = −0.671). The amounts of block due to the fast and slow components are shown as Fast and Slow. The fraction of channels unbound to the fast site (site 1) is 1 − Fast. The fraction of channels unbound to the slow site (site 3) is Unblocked/(Unblocked + Slow). The fraction of channels unbound to site 1 and site 3 is Unblocked = 1 − Fast − Slow. (The washout should have two exponentials; however, we see only one, for two possible reasons. First, the washout is faster than the slow component of wash-in, making it hard to distinguish two components. Second, of the channels that are bound at site 1, half are also bound at site 3. This lowers the number of channels that can contribute to a fast component of washout.) (*B*) Membrane voltage was held at −80 mV and was stepped for 30 ms to 0 mV at 0.2 Hz. Switching external solution from 2 mM K^+/112 mM Na^+ to 10 mM Ba^{2+}/2 mM K^+/92 mM Na^+ for a brief period of time (*solid bar*) caused a quickly relievable block of current. (*C*) Voltage dependence of block for the fast and slow components of Ba^{2+} wash-in. The fraction unblocked of the fast component was calculated as in *A* (Fraction unblocked fast = 1 − Fast) and plotted against step potential. This is the fraction of channels that are unbound to site 1. The values for $K_{d_{fast}}$ and δ_{fast} for the fast component are 10.0 mM and 0.18, respectively, which were obtained from the fit to the equation: Fraction unblocked fast = $(1 + [Ba^{2+}]e^{-\delta fast\ FV2/RT}/K_{d_{fast}})^{-1}$. (see Materials and Methods). The fraction of channels that were not blocked at site 1 or site 3 was calculated as in *A* (Total Unblocked = 1 − Fast − Slow) and plotted against step potential. The values of $K_{d_{slow}}$ and δ_{slow} for the slow component are 1.11 mM and 0.38, respectively, which were obtained from the fit to the equation Total Unblocked fraction = $(1 + [Ba^{2+}]e^{-\delta_{fast}}FV2/RT/K_{d_{fast}} + [Ba^{2+}]e^{-\delta_{slow}\ FV2/RT}/K_{d_{slow}})^{-1}$, where $K_{d_{fast}}$ and δ_{fast} were used from the fit to the fraction unblocked of the fast component. $K_{d_{fast}}$ and $K_{d_{slow}}$ are the Ba^{2+} dissociation constants at 0 mV, and δ is the fraction of the membrane electric field traversed by Ba^{2+} from the external solution to its binding site. Solid lines are fits to the above equations. Membrane voltage and external solutions were controlled as in *A*. (*D*) Determination of closed channel Ba^{2+} off rate. Ba^{2+} off rates were determined from single exponential fits to the Ba^{2+} wash-out. This protocol gives Ba^{2+} dissociation from both open and closed channels; however, the contribution to the total off rate (open plus closed channel) from the open channels decreases with shortening of the step duration. The linear regression extrapolated value of the Ba^{2+} off rate at 0 step duration is the closed-channel off rate (0.01322 s^{-1}).

a deep, slowly equilibrating site, which are sequential in the pore (i.e., a shallow fast site and a deep slow site). This idea was supported by an examination of the dependence of the two components on the step potential. The electrical distance from the external solution to the Ba^{2+} ion binding sites (δ) was smaller for the fast site (0.18) than for the slow site (0.38) (Fig. 5 *C*). Because the fast Ba^{2+} block site is situated shallowly in the membrane electric field, we concluded that this is likely to be the "lock-in" site, and because the slow block site lies deep in the membrane electric field, we concluded that this is likely to be the deep Ba^{2+} binding site. The δ for the deep site (0.38) is very close to the δ_{off} (0.37) observed in the open channel off rate. This indicates that the majority of the voltage dependence for Ba^{2+} binding is in the off rate at this site.

Closed channel unblock of wild-type ShBΔ

The fact that the fraction unblocked for both fast and slow block increased with greater step depolarization indicates that significant Ba^{2+} dissociation occurs during the brief step (i.e., from the open state). Therefore the total Ba^{2+} dissociation rate reflects unbinding from both open channels during the step and closed channels during the interval between steps. To estimate the closed channel Ba^{2+} off rate from its deep binding site, the duration of the step potential was decreased over a range from 90 to 20 ms (Fig. 5 *D*). As the step duration is decreased, the contribution of open channels to the total Ba^{2+} off rate (open plus closed channels) is decreased. Extrapolation of the linear regression fit of the Ba^{2+} off rate versus step duration to 0 ms gives the upper limit of the Ba^{2+} off rate for closed channels at the -80 mV holding potential. This value is the upper limit, because some Ba^{2+} dissociation will occur during the tail. This value was 60-fold slower than the extrapolated value of the open channel off rate from the deep site at -80 mV. This suggests either that opening of the activation gate admits internal K^+, which knocks Ba^{2+} in the outward direction, accelerating the exit of Ba^{2+} from the channel, or that a conformational change in the pore caused by opening lowers an energetic barrier that is rate-limiting for outward Ba^{2+} dissociation.

C-type inactivation traps Ba^{2+} in the pore of wild-type channels

Recent studies have suggested that C-type inactivation occurs by the squeezing shut of the outer mouth of the pore (Yellen et al., 1994; Liu et al., 1996) after the evacuation of a K^+ binding site with an affinity of 2 mM (Baukrowitz and Yellen, 1995, 1996). We asked whether the C-type inactivation gate is analogous to the activation gate (Armstrong and Hille, 1972) in pinching off the outer end of the conduction pathway, rather than producing a general collapse of the pore. We tested this by loading Ba^{2+} into its deep binding site, inducing C-type inactivation, washing external Ba^{2+} away, and then examining whether conduction returned with the kinetics of recovery from C-type inactivation, or with the relatively slower kinetics of Ba^{2+} dissociation.

Channels were blocked by exposure to external Ba^{2+}, and the membrane was held at 0 mV to induce C-type inactivation. Ba^{2+} was then removed from the external solution, and the membrane was held at 0 mV for an additional 10 min. This 10-min wash-out period represents 4000 times the time constant of open channel Ba^{2+} dissociation at 0 mV (K_{off} 0 mV = 6.65 s^{-1}). This should permit all of the channels to recover from block, unless closure of the C-type inactivation gate prevents dissociation of the bound Ba^{2+}. After the wash-out period, the membrane was returned to -80 mV and stepped for short pulses to 0 mV, as before, to test the conducting state of the channels. If C-type inactivation does not retard outward Ba^{2+} dissociation at all, the channels should all lose their Ba^{2+} during the 10-min wash-out, and the current should recover with the kinetics of recovery from C-type inactivation ($\tau = 12.9 \pm 1.05$ s, $n = 11$; Fig. 6). Instead, after the 10-min wash-out of Ba^{2+}, channels recovered monoexponentially with a $\tau = 63.8 \pm 4.5$ s ($n = 11$), fivefold ($p < 1 \times 10^{-9}$) more slowly than recovery from C-type inactivation alone. We observed a similar rate of 63.2 ± 4.6 s ($n = 7$) when we monitored recovery with the same protocol, but omitting the long step to 0 mV that induced C-type inactivation. This demonstrates that the ShBΔ channel can close its C-type inactivation gate with Ba^{2+} occupying the deep site and trap Ba^{2+} in the pore.

Mutations in the P-region affect the binding of Ba^{2+}

In an effort to identify the molecular constituents of the Ba^{2+} and K^+ binding sites, mutations were made in the P-region of ShBΔ. We focused our mutagenesis on the polar residues in the K^+ channel "signature sequence" (Heginbotham et al., 1994). Not all mutants produced functional

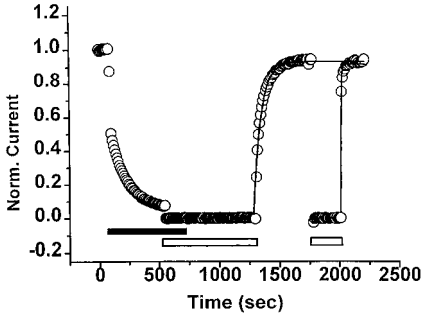

FIGURE 6 C-type inactivation slows Ba^{2+} dissociation from its deep site in wild-type ShBΔ channels. Perfusion of 10 mM Ba^{2+}_{out} (*solid bar*) and switch from $V_{hold} = -80$ mV with steps to 0 mV to $V_{hold} = 0$ mV (*open bar*) to induce C-type inactivation. After 10 min of wash-out of Ba^{2+} at 0 mV, holding the channels in the C-type inactivated state, $66.5 \pm 0.02\%$ ($n = 4$) of the channels recovered and conducted in 50 s, compared to 100% ($n = 4$) of the channels conducting 50 s after a 0-mV depolarization for 3 min in 0 Ba^{2+}.

channels. Of the mutations made, T439Y, Y445C, D447N, and D447T did not give functional homomultimers, whereas T441C, V443G, and Y445F did. Mutations T441C and Y445F preserved selectivity for K^+ over Na^+ (not shown), whereas V443G destroyed channel selectivity, as has been shown earlier (Heginbotham et al., 1994). Cysteines substituted at each of these positions (T441, V443, and Y445) have been shown earlier to be accessible to either internal or external thiol reagents, suggesting that the native residues face the permeation pathway (Lu and Miller, 1995; Pascual et al., 1995).

T441C greatly reduced the slow component of Ba^{2+} block (from 63% to 19%, $p < 10^{-5}$; Fig. 7 *A*), whereas the amount of fast block remained unaffected. This suggests that the external end of the channel, where fast block occurs, was not altered by the mutation, but that a region deep in the pore, where slow block occurs, was affected. The fact that the residual slow component of wash-out of Ba^{2+} was twofold faster ($p = 0.046$) and the fraction slow block was much less for the mutation than for wild-type ShBΔ, indicates that the Ba^{2+} affinity for the deep binding site was decreased because of destabilization of Ba^{2+} binding.

V443G accelerated the kinetics of block without altering the total fraction bound (Fig. 7 *B*). One possibility is that, unlike T441C, which altered binding of Ba^{2+} at its deep site, V443G left binding normal, but eased the entry and exit of Ba^{2+} to and from the deep site, by reducing an energy barrier to Ba^{2+} movement. However, we cannot distinguish this model from a more complex model in which both the deep and shallow sites are altered, with an increased affinity of the shallow site and a decreased affinity of the deep site.

C-type inactivation with Ba^{2+} in the pore of Y445F channels

Y445F had a fast component of block similar to wild-type ShBΔ and an increased sensitivity to slow block (Fig. 7 *C*). This increase in affinity was due to a dramatic (60-fold, $p < 0.01$) slowing of Ba^{2+} dissociation, evident in the wash-out. This mutant also exhibited an unusually fast C-type inactivation (Fig. 8 *A*). Recovery from this inactivation was slow enough so that, unlike wild-type ShBΔ, 5-s intervals at −80 mV were insufficient to prevent accumulation of inactivation during the repeated 30-ms steps (Fig. 8 *B*). This raised the possibility that the apparent increase in the Ba^{2+} affinity of site 3 is actually due to trapping of Ba^{2+} at that site by closure of the C-type inactivation gate. We examined this possibility further.

Increasing external K^+ from 2 mM to 112 mM slowed C-type inactivation in Y445F by sixfold (Fig. 8 *A*), comparable to the effect observed in wild-type ShB and ShBΔ channels (Lopez-Barneo et al., 1993; Baukrowitz and Yellen, 1996). This indicates that the K^+ site that influences C-type inactivation in Y445F is intact. To determine if the fast closure of the C-type inactivation gate in Y445F was responsible for the slow time course of Ba^{2+} wash-out rate, we compared Ba^{2+} wash-out in low and high external $[K^+]$. If the slow wash-out of Ba^{2+} from Y445F channels was due to the channel C-type inactivating on Ba^{2+}, then Ba^{2+} wash-out should be faster in 112 mM K^+_{out}, where C-type inactivation is slowed. Indeed, the rate of Ba^{2+} wash-out was 14-fold ($p = 2 \times 10^{-2}$) faster when external K^+ was raised to 112 mM compared to 2 mM (Fig. 8 *C*).

The increase in the rate of Ba^{2+} dissociation in high K^+_{out} could not have been due to enhanced Ba^{2+} inward dissociation, because dissociation was faster at +80 mV than at +20 mV (Fig. 9 *A*). This voltage dependence indicates that the bulk of the Ba^{2+} dissociations for Y445F in 112 mM K^+_{out} were in the outward direction. This is in contrast to wild-type ShBΔ channels, where 112 mM K^+_{out} accelerates inward dissociation (Fig. 3 *B*). This result suggests that the "enhancement" site is disrupted in Y445F channels, whereas the preservation of fast Ba^{2+} block, as shown above, suggests that the "lock-in" site remains intact.

Mutation Y445F lowers the affinity of a K^+ ion binding site

To test the above interpretation that Y445F disrupts the "enhancement" site, we compared wild-type ShBΔ and Y445F with respect to the onset of Ba^{2+} block in high external K^+. This test was motivated by the results of Hurst et al. (1995), which showed that high external K^+ eliminates the slow component of Ba^{2+} block and attenuates the fast component in N-terminal deleted ShH4 channels, an observation that we repeated (Fig. 9 *B*). This result suggests that high K^+ occupancy of the "enhancement" site or the deep Ba^{2+} binding site prevents external Ba^{2+} from reaching the deep site. In contrast to wild-type ShBΔ, Y445F preserved both the fast and slow components of block in 92 mM K^+_{out}, although both were reduced in magnitude and in rate compared to 2 mM K^+_{out} (compare Figs. 7 *C* and 9 *C*). This indicates that in Y445F channels Ba^{2+} can reach its deep site, even in 92 mM K^+_{out}, and is consistent with a decreased occupancy of a low-affinity K^+ binding site in Y445F channels. Because the fast and slow Ba^{2+} binding sites were intact in Y445F channels (although the affinity of the deep site could not be ascertained because of the trapping by C-type inactivation), the low-affinity K^+ binding site affected by this mutation seemed most likely to be the "enhancement" site.

DISCUSSION

Ion binding sites

Our results on the *Shaker* channel are consistent with the existence of at least three single-file permeant ion binding sites in the pore that can be simultaneously occupied. All of these sites are in exchange with the external solution when the activation gate is closed. As shown earlier for BK channels (Neyton and Miller, 1988a, b), we find for *Shaker* that low concentrations of external permeant ion slow out-

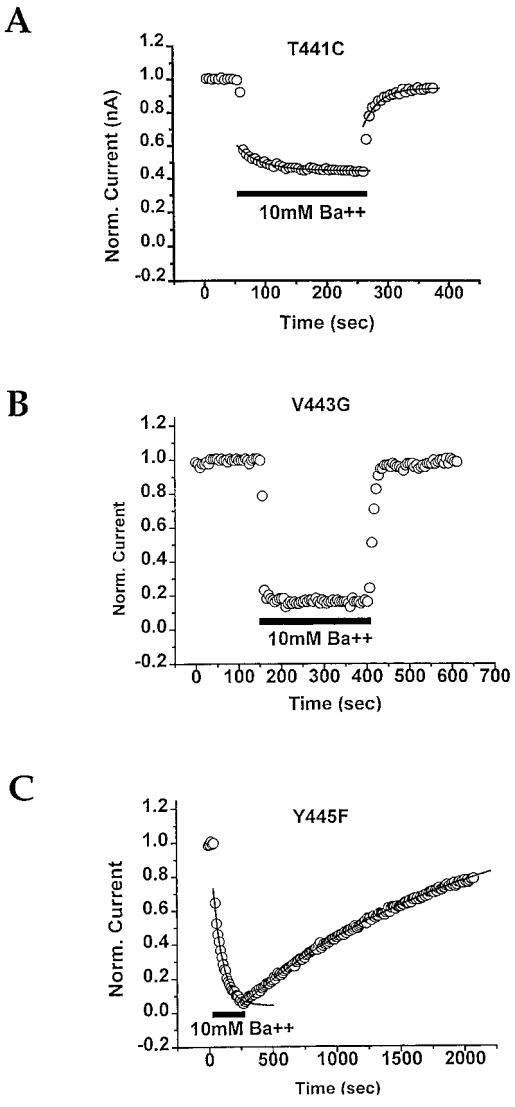

FIGURE 7 Mutations in the P-region affect barium block. Solutions are 0 Ba^{2+} (2 mM K^+/112 mM Na^+/0 Ba^{2+}) and 10 mM Ba^{2+} (2 mM K^+/92 mM Na^+/10 mM Ba^{2+}). The fraction unblocked of the fast component was measured as the fraction of the total current in the absence of Ba^{2+} after equilibration of the fast component as in Fig. 5 *C* (Fraction unbound Fast = 1 − Fast). Fraction unblocked of the slow component was measured as the current value at steady state, expressed as a fraction of the current remaining after fast block (Unblocked/Unblocked + Slow). (*A*) Mutation T441C had a fast Ba^{2+} block similar to that of wild-type ShBΔ (T441C Fraction unblocked = 0.566 ± 0.024, $n = 6$; wild-type ShBΔ Fraction unblocked = 0.650 ± 0.013, $n = 6$); however, the fraction unblocked of the slow component was significantly increased ($p = 1 \times 10^{-5}$) for T441C (0.813 ± 0.042, $n = 3$) compared to wild-type ShBΔ (0.375 ± 0.0313, $n = 6$). The time constant for the slow component of wash-in is 32.7 ± 11.71 s ($n = 2$). The time constant for wash-out for T441C is 17.00 ± 4.98 s ($n = 3$), which is significantly shorter ($p = 4.56 \times 10^{-2}$) than that of wild-type ShBΔ (27.86 ± 1.75 s, $n = 6$). The amplitudes for the wash-in and wash-out of the slow component were 0.10 ± 0.02 and 0.21 ± 0.076 ($n = 2$), respectively ($V_{hold} = -80$ mV; $V_{step} = +40$ mV). (*B*) Mutation V443G increased Ba^{2+} blocking kinetics so much that the time constants of block could not be determined. Fraction unblocked = 0.126 ± 0.056 ($n = 2$) ($V_{hold} = -100$ mV; $V_{step} = +40$ mV). (*C*) The mutation Y445F had both fast and slow ($\tau = 69.1 \pm 8.63$ s; amp = 0.625 ± 0.069; $n = 5$) components of block for Ba^{2+} wash-in. The fraction unblocked for the fast component for Y445F 0.610 ± 0.0239 ($n = 7$) was comparable ($p = 0.173$) to wild-type ShBΔ 0.650 ± 0.0149 ($n = 7$); however, the slow component was slower and had a smaller fraction unblocked. The fraction unblocked of the slow component for Y445F was 0.101 ± 0.0227 ($n = 7$), which is significantly smaller ($p < 10^{-5}$) than wild-type ShBΔ 0.395 ± 0.0282 ($n = 7$). The Ba^{2+} wash-out was significantly slower ($p < 0.01$) for Y445F (1670 ± 390 s, $n = 8$) compared to 27.9 ± 1.75 s ($n = 5$) for wild-type ShBΔ ($V_{hold} = -80$ mV; $V_{step} = +40$ mV).

ward Ba^{2+} dissociation, and high concentrations drive Ba^{2+} inward, except at very strong depolarizations. Neyton and Miller referred to these two permeant ion effects as "lock-in," which they attributed to block of the pathway for Ba^{2+} outward dissociation from its deep site due to occupancy of a distal site, and "enhancement," which they attributed to repulsion of Ba^{2+} in the inward direction out of its binding site due to occupancy of a nearby site. Such repulsion of a blocker by a permeant ion has also been observed in BK channels by other workers (Yellen, 1984) and in the delayed rectifier of the squid giant axon (Bezanilla and Armstrong, 1972). Because the repulsion is mutual, binding of the permeant ion to the "enhancement" site is unfavorable when the deep site is occupied by Ba^{2+}, so that this only occurs at high external concentration of permeant ion. A simple model that incorporates these principles accounted well for the voltage dependence of open channel Ba^{2+} dissociation in three different external K^+ concentrations (see below).

Our results indicate that the "lock-in" site is highly selective for permeant ions, suggesting that it lies within the permeation pathway. Because it can also be occupied by Ba^{2+}, it is most likely the shallow site ($\delta = 0.18$) that rapidly equilibrates with extracellular Ba^{2+} before Ba^{2+} goes deeper into the pore and binds tightly to its deeper site ($\delta = 0.38$). This is in agreement with the earlier results of Hurst et al. (1995). Both the electrical location of the "lock-in" site, and the site's affinity for K^+ predicted from the fit of our three binding site model ($K_d = 0.75$ mM; see below), are quantitatively similar to measurements on BK channels ($\delta = 0.15$, $K_d = 0.3$ mM; Neyton and Miller, 1988a, b). (It should be noted that in our experiments and in the studies of Neyton and Miller, the affinity of the "lock-in" site is measured with a Ba^{2+} already bound to the deep site. This might cause the affinity of the K^+ site to be less than if Ba^{2+} was not present because of any repulsion between the ions; however, we do not think this is so. See below.) The selectivity series of the "lock-in" site is also similar between these channels ($Rb^+ > K^+ > NH_4^+$), except that *Shaker* appears to be more selective against Na^+. Replacing 112 mM Na^+_{out} with 112 mM $NMDG^+_{out}$ had little effect on the Ba^{2+} off rate for ShBΔ, whereas Neyton and Miller (1988a) observe a fourfold increase in the Ba^{2+} off rate when Na^+ is replaced with $NMDG^+$.

The K^+ affinity of the "enhancement" site is also similar between these two channels, requiring over 100 mM external K^+ to raise occupancy to the point that inward Ba^{2+} dissociation is favored at modest depolarizations. The voltage dependence of the off rate for outward and inward Ba^{2+} dissociation was also similar for the two channels. For outward dissociation in 0 mM K^+_{out}, the δ_{off} for BK was 0.42

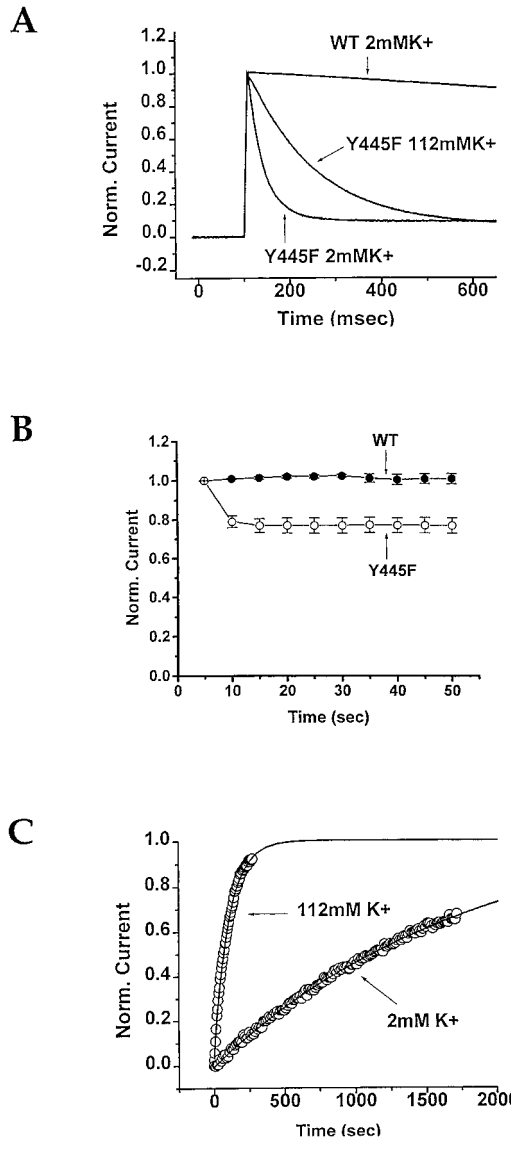

FIGURE 8 Y445F channels can C-type inactivate with a Ba^{2+} ion in the pore. (*A*) Mutation Y445F increases the rate of C-type inactivation compared to wild-type ShBΔ. The time constant for inactivation in 2 mM K^+_{out} for wild-type ShBΔ (4190 ± 93.9 ms, $n = 4$) was 150-fold ($p < 1 \times 10^{-11}$) slower than that of Y445F (25.2 ± 3.81 ms, $n = 6$). For Y445F the time constant for inactivation in 2 mM K^+_{out} was significantly faster ($p < 1 \times 10^{-7}$) than 112 K^+_{out} (144 ± 9.58 ms, $n = 6$) ($V_{hold} = -80$ mV; $V_{step} = +40$ mV). (*B*) The membrane voltage was held at −80 mV and stepped to +40 mV for 30 ms at 0.2 Hz. Repeated depolarizations cause a decrease in Y445F current, unlike in wild-type ShBΔ. This is probably due to accumulated C-type inactivation in Y445F. (*C*) Ba^{2+} wash-out of Y445F is faster ($p < 0.05$) with 112 mM K^+_{out} ($\tau_{off} = 116 \pm 19.3$ s, $n = 4$) than 2 mM K^+_{out} ($\tau_{off} = 1670 \pm 390$ s, $n = 8$), suggesting that 112 mM K^+_{out} slows C-type inactivation, allowing Ba^{2+} to dissociate more quickly ($V_{hold} = -80$ mV; $V_{step} = +40$ mV).

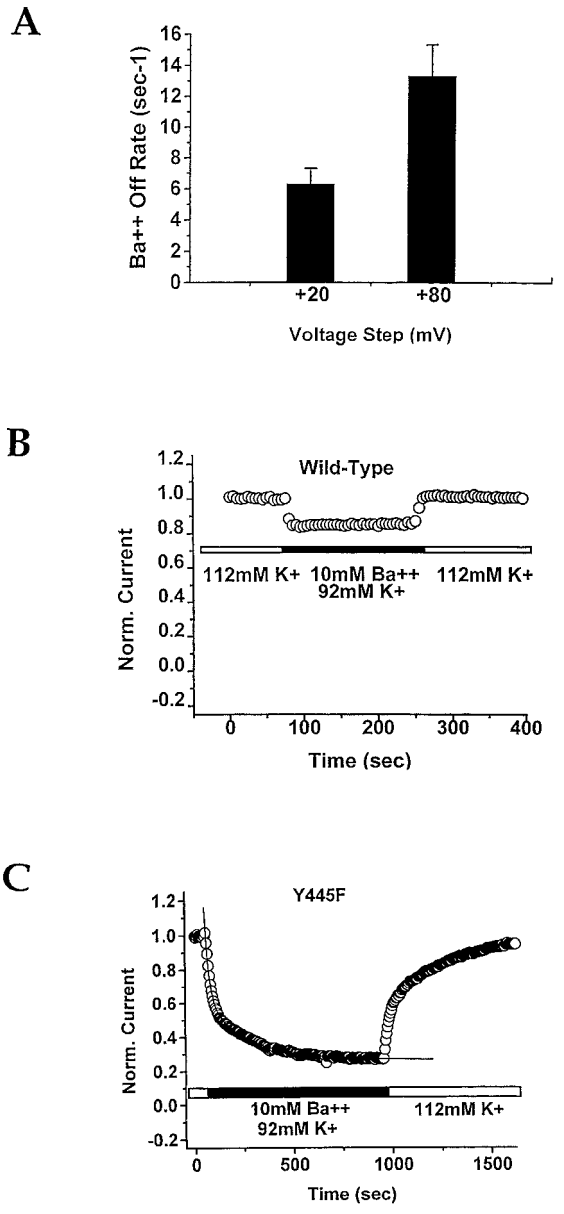

FIGURE 9 Mutation Y445F disrupts a K^+ ion binding site. (*A*) Ba^{2+} off rates for Y445F were significantly faster ($p < 0.01$) for steps to +80 mV ($n = 9$) than +20 mV ($V_{hold} = -80$ mV; $V_{step} = +40$ mV; step duration = 30 ms; 0.2 Hz). (*B*) Absence of slow Ba^{2+} block in wild-type ShBΔ channels in 112 mM K^+_{out} ($V_{hold} = -80$ mV; $V_{step} = +40$ mV). (*C*) Wash-in of Ba^{2+} has two components for Y445F in 112 mM K^+_{out} ($\tau_1 = 19.6 \pm 0.847$ s; $amp_1 = 0.618 \pm 0.028$; $\tau_2 = 232.9 \pm 19.4$ s; $amp_2 = 0.284 \pm 0.026$; $n = 7$).

and the δ_{off} for ShBΔ was 0.35. For inward dissociation the δ_{off} was 0.32 for BK (150 mM K^+_{out}) and 0.34 for ShBΔ (112 mM K^+_{out}). These results demonstrate that there is a high degree of conservation of pore structure between these subfamilies of K^+ channels.

Three ion binding site model

A simple three binding site model (see Materials and Methods) of the *Shaker* pore, of the kind proposed qualitatively by Neyton and Miller for the BK channel (1988a, b), accounted well for the observed voltage dependence of open channel Ba^{2+} dissociation in the three different external K^+ concentrations. The "lock-in" site has the experimentally determined electrical position of the fast Ba^{2+} site of 0.18. The "enhancement" site lies between the "lock-in" site and

the deep, slow Ba^{2+} binding site, which has the experimentally determined electrical position of 0.38.

Wash-in and prolonged wash-out of external Ba^{2+} from closed channels at negative voltage leaves one Ba^{2+} loaded in the deep Ba^{2+} site, whereas Ba^{2+} is washed out of the "lock-in" and "enhancement" sites, where it binds weakly. (Ba^{2+} is held weakly at the "lock-in" site because of its rapid equilibration (Fig. 5 *A*), and repulsion by Ba^{2+} at the deep site prevents a second Ba^{2+} from binding tightly at the nearby "enhancement" site.) Therefore, when the external solution is devoid of external K^+, the "lock-in" and "enhancement" sites are vacant. At 2 mM external K^+ concentration, K^+ occupies the "lock-in" site a large fraction of the time, blocking the pathway for outward Ba^{2+} dissociation from the deep site, so that the Ba^{2+} must wait until the "lock-in" site is vacated before it can exit. Repulsion by Ba^{2+} at its deep site prevents K^+ from occupying the "enhancement" site at low external $[K^+]_{out}$. However, when external K^+ concentration is raised to 112 mM (56-fold higher), the "enhancement" site becomes significantly occupied. The mutual repulsion between the K^+ at the "enhancement" site and Ba^{2+} at its deep site drives Ba^{2+} in the inward direction.

Simultaneous fits of the model to the curves relating open channel Ba^{2+} off rate to voltage in 0, 2, and 112 mM $[K^+]_{out}$ fit the data well (Fig. 3 *B, solid lines*). The affinity of the "lock-in" site for K^+ predicted from fits of our three binding site model (K_d = 0.75–0.80 mM) agrees well with that measured BK channels (K_d = 0.3 mM; Neyton and Miller, 1988a).

The C-type inactivation gate is external to the deep Ba^{2+} binding site

Armstrong et al. (1982) showed that Ba^{2+} can enter the closed delayed rectifier K^+ channel from the outside and bind with high affinity at its blocking site. Armstrong et al. also showed that internal Ba^{2+} was prevented from access to its binding site when the activation gate was closed. This indicated that activation gating operates by opening and closing access of the pore to ions in the internal solution. We find here that another gate, the C-type inactivation gate, can function in a similar manner from the opposite end of the pore. Access to the external solution of a Ba^{2+} ion bound at its deep site in the pore was cut off by closure of the C-type inactivation gate. This indicates that the C-type inactivation gate pinches off the permeation pathway between the deep Ba^{2+} site and the external mouth of the pore, and suggests that C-type inactivation does not produce a general collapse of the pore. The rearrangement that brings residues in the P-S6 of one subunit closer to those of another when the C-type inactivation closes (Liu et al., 1996) seems to therefore represent a local structural event. Recent work by Molina et al. (1997) suggests that the pinching off is internal to residue T449, which places the C-type inactivation gate between T449 and T441, the deep Ba^{2+} binding site.

The rate of C-type inactivation depends on the external concentration of K^+ (Lopez-Barneo, 1993; Baukrowitz and Yellen, 1995, 1996). Using organic blockers with differing bound times at the internal mouth of the channel, Baukrowitz and Yellen (1996) showed that block of outward current flow increased the sensitivity of C-type inactivation to external K^+, consistent with the idea that if a K^+ ion that dissociates from the pore is not replaced by flux from the internal solution, then the C-type inactivation gate can close. To account for the long apparent dwell time (150 μs) of the K^+ ion at the C-type inactivation site, Baukrowitz and Yellen proposed that this ion must not experience repulsion by other ions in the pore, that is, that it must be the last ion in the pore. We find that even after the C-type inactivation K^+ ion has dissociated, permitting closure of the gate, a Ba^{2+} ion can remain at the deep site. This suggests that the repulsion between a K^+ ion at the deep site and another K^+ ion at the C-type inactivation site must be weak. In fact, we find that K^+ has a high affinity for the "lock-in" site, even with Ba^{2+} at the deep site. Moreover, with K^+ at the "lock-in" site, at voltages near zero, Ba^{2+} dissociation from the deep site is still preferentially in the outward direction, providing no evidence for repulsion between these sites. Certainly, whatever repulsion exists between the "lock-in" site and the deep site must be much weaker than what we observe between the deep site and the "enhancement" site.

The binding site that must be evacuated for the C-type inactivation gate to close has a K^+ affinity (K_d = 0.5–2 mM; Lopez-Barneo et al., 1993; Baukrowitz and Yellen, 1996) similar to that of our "lock-in" site (K_d = 0.75 mM), suggesting that it may be the same site, if there is little repulsion between the deep site and the "lock-in" site, as mentioned above. Such a superficial location of the "lock-in" site would explain how pinching off the area around the C-type inactivation K^+ binding site could prevent outward dissociation of Ba^{2+} from the deep site.

Molecular determinants of ion binding sites

At the level of primary structure the greatest identity in pore forming domains between *Slo,* which encodes the BK channel, and *Shaker* is in the "signature sequence" of the P-region, which has been implicated in forming the narrowest part of the pore, and the selectivity filter (Heginbotham et al., 1992, 1994; Kurz et al., 1995; Lu and Miller, 1995; Pascual et al., 1995). Our mutagenesis suggests that residues in the signature sequence contribute to the region of the permeant ion binding sites studied above.

T441C decreased the affinity of the slow Ba^{2+} block site by increasing the Ba^{2+} off rate, without affecting the affinity of the fast block site. This is consistent with a localized change at the deep site. This result is in agreement with recent results on the inward rectifier ROMK2, in which substitution of a threonine at the analogous position increases Ba^{2+} block (Zhou et al., 1996). The finding suggests

that there is a conservation of pore architecture between the widely divergent inward rectifier K^+ channels and the voltage-gated K^+ channels. T441 may contribute its hydroxyl to the deep site, or alternatively, the T441 side chain may influence the neighboring position T442, which has been modeled to contribute its backbone carbonyl to form a K^+ binding site (Durell and Guy, 1996).

V443G accelerated block kinetics even more than T441C, but preserved the overall steady-state level of Ba^{2+} block. The Ba^{2+} wash-out rate was slower than the wild-type ShBΔ fast dissociation, which we associate with the "lock-in" site, and faster than the wild-type ShBΔ deep site dissociation. These results could be accounted for if the Ba^{2+} bound at the deep site state were unaffected by the mutation, but the rate of movement between the external solution and the deep site was accelerated by the reduction of an energy barrier to ion movement. Because V443G destroys selectivity (Heginbotham et al., 1994), it is possible that it is the selectivity filter that constitutes such an energy barrier, perhaps involving a constriction in the pore at or near this site.

The mutation Y445F eliminated enhancement of inward Ba^{2+} dissociation in high external K^+. The high-affinity K^+ binding site whose occupancy controls C-type inactivation was normal in this mutant, in that raising external K^+ from 2 to 112 mM slowed inactivation by sixfold (Fig. 7 *A*), similar to the effect shown earlier for wild-type channels (Baukrowitz and Yellen, 1996). Because two properties that we associate with the "lock-in" site—high-affinity K^+ binding and fast Ba^{2+} block—were unaffected, we think that the mutation Y445F does not affect the "lock-in" site. Because the low-affinity K^+ binding site that determines both the direction of Ba^{2+} dissociation from the deep site and the ability of external Ba^{2+} to reach the deep site in high $[K^+]_{out}$ was disrupted, but the deep site was intact, we conclude that the mutation disrupts the "enhancement" site. This conclusion is consistent with the work of Ranganathan et al. (1996), which showed that Y445F disrupts a K^+ ion binding site near the external mouth of the pore. It also supports the model of Durell and Guy (1996), in which the hydroxyl group of Y445 acts as a coordination site for K^+.

CONCLUSION

Our results show that three binding sites, in ready exchange with external permeant ions, are located in a stretch of the *Shaker* pore where the outer 40% of the electric field drops. The success of our three-site model in fitting our measured voltage dependence of Ba^{2+} dissociation indicates that the appealingly straightforward ideas of "lock-in" and "enhancement," coined by Neyton and Miller (1988a, b) for the BK channel, can account for flux interactions in the deep pore of the *Shaker* K^+ channel.

The two deeper sites, the "enhancement" site and the deep site, and what may be a constriction between them that both retards ion movement and contributes to selectivity,

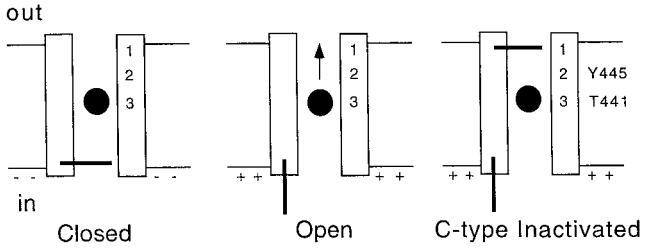

FIGURE 10 Model of ion binding sites relative to the activation and C-type inactivation gates. At negative voltages, Ba^{2+} is pulled inward by the electric field, but inward Ba^{2+} dissociation is prevented by closure of the activation gate. At positive voltages Ba^{2+} is pushed outward by the field and is free to dissociate into the external solution when the channel is open, but is blocked by the closure of the C-type inactivation gate. Y445F lowers the affinity of K^+ for the "enhancement" site (site 2), T441C lowers the affinity of Ba^{2+} for the deep site (site 3), and V443G lowers an energetic barrier between the external "lock-in" site and the deep Ba^{2+} block site.

appear to be formed by a short stretch of five amino acids in the most conserved portion of the P-region (Fig. 10). The "enhancement" site and the deep site are close enough so that mutual repulsion during their simultaneous occupancy accelerates dissociation. This confirms one of the key features of the long multiion pore proposed by Neyton and Miller (1988b), which allows these highly selective channels to flux ions at such high rates. A third binding site, which appears to correspond to the one that must be empty for the C-type inactivation gate to pinch off the conduction pathway, is located closer to the external mouth of the channel. Because the residues that we have studied appear to be the ones in the P-region that protrude furthest toward the internal side of the pore (Lu and Miller, 1995; Pascual et al., 1995), this suggests that about half of the electrical depth of the pore is formed by domains outside of H5, such as S4–S5 and S6.

We thank Oliver Baker and Harold Lecar for helpful discussion of the manuscript.

This work was supported in part by the McKnight Endowment Fund for Neuroscience and the American Heart Association (96-248A). HPL was supported by the Wenner-Gren Foundation, and REH was supported by a National Institutes of Health training grant (GM08295).

REFERENCES

Aiyar, J., A. Nguyen, K. Chandy, and S. Grissmer. 1994. The P-region and S6 of Kv3.1 contribute to the formation of the ion conduction pathway. *Biophys. J.* 67:2261–2264.

Aiyar, J., J. Withka, J. Rizzi, D. Singleton, G. Andrews, W. Lin, J. Boyd, D. Hanson, M. Simon, B. Dethlefs, C. Lee, J. Hall, G. Gutman, and K. Chandy. 1995. Topology of the pore-region of a potassium channel revealed by the NMR-derived structures of scorpion toxins. *Neuron.* 15:1169–1181.

Armstrong, C., and B. Hille. 1972. The inner quaternary ammonium ion receptor of potassium channels of the node of Ranvier. *J. Gen. Physiol.* 59:388–400.

Armstrong, C., R. Swenson, Jr., and S. Taylor. 1982. Block of squid axon potassium channels by internally and externally applied barium ions. *J. Gen. Physiol.* 80:663–682.

Baukrowitz, T., and G. Yellen. 1995. Modulation of potassium current by frequency and external [K+]: a tale of two inactivation mechanisms. *Neuron.* 15:951–960.

Baukrowitz, T., and G. Yellen. 1996. Use-dependent blockers and exit rate of the last ion from the multi-ion pore of a potassium channel. *Science.* 271:653–656.

Bezanilla, F., and C. Armstrong. 1972. Negative conductance caused by entry of sodium and cesium ions into the potassium channels of squid axons. *J. Gen. Physiol.* 60:588–608.

Choi, K., C. Mossman, J. Aube, and G. Yellen. 1993. The internal quaternary ammonium receptor site of Shaker potassium channels. *Neuron.* 10:533–541.

Durell, S., and H. Guy. 1996. Structural model of the outer vestibule and selectivity filter of the *Shaker* voltage-gated potassium channel. *Neuropharmacology.* 35:761–773.

Goldstein, S., D. Pheasant, and C. Miller. 1994. The charybdotoxin receptor of a *Shaker* K^+ channel: peptide and channel residues mediating molecular recognition. *Neuron.* 12:1377–1388.

Harris, R., and E. Isacoff. 1996. Hydrophobic mutations alter the movement of magnesium in the pore of voltage-gated potassium channels. *Biophys. J.* 71:209–219.

Hartmann, H., G. Kirsh, J. Drewe, M. Taglialatela, R. Joho, and A. Brown. 1991. Exchange of conduction pathways between two related potassium channels. *Science.* 251:942–944.

Heginbotham, L., T. Abramson, and R. MacKinnon. 1992. A functional connection between the pores of distantly related ion channels as revealed by mutant K^+ channels. *Science.* 258:1152–1155.

Heginbotham, L., Z. Lu, T. Abramson, and R. MacKinnon. 1994. Mutations in the K^+ channel signature sequence. *Biophys. J.* 66:1061–1067.

Heginbotham, L., and R. MacKinnon. 1992. The aromatic binding site for TEA^+ ion on potassium channels. *Neuron.* 8:483–491.

Hidalgo, P., and R. MacKinnon. 1995. Revealing the architecture of a K^+ channel pore through mutant cycles with a peptide inhibitor. *Science.* 268:307–310.

Hille, B. 1992. Ionic Channels of Excitable Membranes. Sinauer Associates, Sunderland, MA.

Hodgkin, A., and R. Keynes. 1955. The potassium permeability of a giant nerve fibre. *J. Physiol. (Lond.).* 128:61–88.

Hoshi, T., W. Zagotta, and R. Aldrich. 1990. Biophysical and molecular mechanisms of *Shaker* potassium channel inactivation. *Science.* 250: 533–538.

Hurst, R., R. Latorre, L. Toro, and E. Stefani. 1995. External barium block of *Shaker* potassium channels: evidence for two binding sites. *J. Gen. Physiol.* 106:1069–1087.

Hurst, R., L. Toro, and E. Stefani. 1996. Molecular determinants of external barium block in Shaker potassium channels. *FEBS Lett.* 388: 59–65.

Isacoff, E. Y., Y. N. Jan, and L. Y. Jan. 1991. Putative receptor for the cytoplasmic inactivation gate in the Shaker K^+ channel. *Nature.* 353: 86–90.

Isacoff, E., G. Lopez, Y. Jan, and L. Jan. 1993. A site near the transmembrane segment S6 of potassium channels interacts with barium ions. *Biophys. J.* 64:A226.

Kirsch, G., J. Drewe, M. Taglialatela, R. Joho, M. DeBaisi, H. Hartmann, and A. Brown. 1992. A single nonpolar residue in the deep pore of related K^+ channels acts as a K^+/Rb^+ conductance switch. *Biophys. J.* 62:136–144.

Kurz, L., and R. Zulke, H. Zhang, and R. Joho. 1995. Side-chain accessibilities in the pore of a potassium channel probed by sulfhydryl-specific reagents after cysteine-scanning mutagenesis. *Biophys. J.* 68:900–905.

Liu, Y., M. Jurman, and G. Yellen. 1996. Dynamic rearrangement of the outer mouth of a potassium channel during gating. *Neuron.* 16:859–867.

Lopez, G. A., Y. N. Jan, and L. Y. Jan. 1994. Evidence that the S6 segment of the *Shaker* voltage-gated K^+ channel comprises part of the pore. *Nature.* 367:179–182.

Lopez-Barneo, J., T. Hoshi, S. Heinemann, and R. Aldrich. 1993. Effects of external cations and mutations in the pore region on C-type inactivation of Shaker potassium channels. *Receptors Channels.* 1:61–71.

Lu, Q., and C. Miller. 1995. Silver as a probe of pore-forming residues in a potassium channel. *Science.* 268:304–307.

MacKinnon, R., L. Heginbotham, and T. Abramson. 1990. Mapping the receptor site for charybdotoxin, a pore-blocking potassium channel inhibitor. *Neuron.* 5:767–771.

MacKinnon, R., and C. Miller. 1989. Mutant potassium channels with altered binding of charybdotoxin, a pore-blocking peptide inhibitor. *Science.* 245:1382–1385.

MacKinnon, R., and G. Yellen. 1990. Mutations affecting TEA blockade and ion permeation in voltage-activated potassium channels. *Science.* 250:276–279.

Miller, C. 1987. Trapping single ions inside single ion channels. *Biophys. J.* 52:123–126.

Miller, C., R. Latorre, and I. Reisin. 1987. Coupling of voltage-dependent gating and barium block in the high conductance, calcium-activated K+ channel. *J. Gen. Physiol.* 90:427–449.

Molina, A., A. Castellano, and J. Lopez-Barneo. 1997. Pore mutations in Shaker potassium channels distinguish between the sites of TEA blockade and C-type inactivation. *J. Physiol. (Lond.).* 499:361–367.

Naranjo, D., and C. Miller. 1996. A strongly interacting pair of residues on the contact surface of charybdotoxin and a *Shaker* potassium channel. *Neuron.* 16:123–130.

Neyton, J., and C. Miller. 1988a. Potassium blocks barium permeation through a calcium-activated potassium channel. *J. Gen. Physiol.* 92: 549–567.

Neyton, J., and C. Miller. 1988b. Discrete barium block as a probe of ion occupancy and pore structure in the high-conductance calcium-activated potassium channel. *J. Gen. Physiol.* 92:569–586.

Neyton, J., and M. Pelleschi. 1991. Multi-ion occupancy alters gating in high-conductance, calcium activated potassium channels. *J. Gen. Physiol.* 97:641–665.

Pascual, J. M., C. Shieh, G. Kirsch, and A. Brown. 1995. K^+ pore structure revealed by reporter cysteines at inner and outer surfaces. *Neuron.* 14:1055–1063.

Ranganathan, R., J. Lewis, and R. MacKinnon. 1996. Spatial localization of the potassium channel selectivity filter by mutant cycle-based structure analysis. *Neuron.* 16:131–139.

Sambrook, J., E. Fritsch, and T. Maniatis. 1989. *Molecular Cloning, 2nd Ed.* Cold Spring Harbor Laboratory, Cold Spring Harbor, NY.

Slesinger, P., Y. Jan, and L. Jan. 1993. The S4–S5 loop contributes to the ion-selective pore of potassium channels. *Neuron.* 11:739–749.

Stampe, P., and T. Begenisich. 1996. Unidirectional K^+ fluxes through recombinant *Shaker* potassium channels expressed in single *Xenopus* oocytes. *J. Gen. Physiol.* 107:449–457.

Taglialatela, M., M. S. Champagne, J. A. Drewe, and A. M. Brown. 1994. Comparison of H5, S6, and H5–S6 exchanges on pore properties of voltage-dependent K^+ channels. *J. Biol. Chem.* 269:13867–13873.

Woodhull, A. 1973. Ionic blockage of sodium channels in nerve. *J. Gen. Physiol.* 61:687–708.

Yellen, G. 1984. Relief of Na^+ block of Ca^{2+}-activated K^+ channels by external cations. *J. Gen. Physiol.* 84:187–199.

Yellen, G., M. Jurman, T. Abramson, and R. MacKinnon. 1991. Mutations affecting internal TEA blockade identify the probable pore-forming region of a potassium channel. *Science.* 251:939–942.

Yellen, G., D. Sodickson, T. Chen, and M. Jurman. 1994. An engineered cysteine in the external mouth of a potassium channel allows inactivation to be modulated by metal binding. *Biophys. J.* 66:1068–1075.

Yool, A., and T. Schwarz. 1991. Alteration of ionic selectivity of a potassium channel by mutation of the H5 region. *Nature.* 349:700–704.

Zhou, H., S. Chepilko, W. Schutt, H. Choe, L. Palmer, and H. Sackin. 1996. Mutations in the pore region of ROMK enhance barium block. *Am. J. Physiol.* 271:C1949–C1956.